

Study of radial transport of tracers in CUTIE

G. Sánchez Burillo¹, B. Ph. van Milligen¹, A. Thyagaraja²

¹ *Laboratorio Nacional de Fusión, EURATOM/CIEMAT, Madrid, Spain*

² *EURATOM/UKAEA Fusion association, Culham Science Centre, Abingdon, UK*

Introduction

Radial transport in fusion grade plasmas is still not fully understood. It has been suggested that the transport of particles and/or heat could be non-diffusive. The probabilistic Continuous Time Random Walk (*CTRW*), provides a framework for the understanding of anomalous transport, and is especially useful when long-range and/or long-time correlations are involved.

CUTIE is a three dimensional full-tokamak fluid turbulence code that incorporates most of the relevant physics. In particular, it models the non-linear back reaction of the turbulence on the macro-scale profiles and vice-versa [1]. Therefore, it is a good test bed for studying anomalous transport using tracer particles. We have studied the motion of such tracers using various techniques, with the main goal of determining α and β , i.e. the decay indexes of the tracer particle distribution functions (pdfs), and the Hurst exponent $H = \beta/\alpha$, in order to clarify whether the effective transport, measured over large distances and long time scales, is either diffusive ($H = \frac{1}{2}$), subdiffusive ($H < \frac{1}{2}$) or superdiffusive ($H > \frac{1}{2}$) [2]. Standard values are $\alpha = 2$ (gaussian), $\beta = 1$ (markovian) and $H = \frac{1}{2}$ (diffusive motion).

Tracer particles

CUTIE provides the fluctuating fluid velocity at grid points. We have modified the code to follow tracer particles in a simulation for COMPASS. We used Fourier oversampling to refine the grid, and then performed 3D spline interpolation to obtain the velocity at any point in space. We then launched 10000 passive and ideal ($q = m = 0$) tracer particles into a converged turbulence simulation. The particles were launched simultaneously at mid radius and randomly distributed along the poloidal and toroidal directions. The total simulation time was $\tau_{\text{Tot}} = 20$ ms, i.e., comparable to the particle confinement time.

Probability distribution functions

Assuming that the tracer motion can be well described by a separable *CTRW* with separate pdfs for the step size ($p(\Delta x)$) and the waiting time ($\psi(\Delta t)$) [3], we decompose the continuous motion into steps and waiting time intervals on the basis of a velocity threshold. Based on the generalized Central Limit Theorem, we expect the pdfs of these steps and waiting times to be Lévy distributions. For $p(\Delta x)$, this would be a symmetric non gaussian stable Lévy distribution,

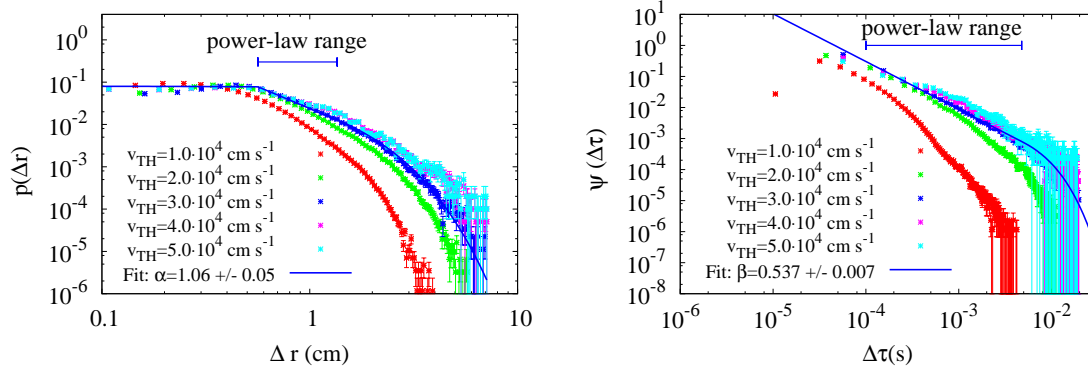


Figure 2: Step size pdf (left) and Waiting time pdf (right) for different v_{TH} . In both cases there exists a region where power-law decay is clearly detected, specially for $v_{TH} = 3 \cdot 10^4$ cm/s.

while for $\psi(\Delta t)$ this would be a fully antisymmetric Lévy distribution due to the asymmetry of the time parameter. These Lévy distributions are characterised by their decay indexes: for large Δx , $p \rightarrow (\Delta x)^{-(1+\alpha)}$, with $0 < \alpha < 2$, and for large Δt , $\psi \rightarrow (\Delta t)^{-(1+\beta)}$, with $0 < \beta < 1$.

Radial distribution of tracers

The radial distribution of tracers should reflect this in the sense that its tail is expected to decay as $p(\Delta x)$, i.e. $\text{pdf}(x) \rightarrow x^{-(1+\alpha)}$. We have calculated this distribution $\text{pdf}(\rho)$ at different times in the simulation times. The temporal evolution of the distribution shows an outward drift. Towards the inside, an algebraic tail is detected. The outward tail is de-

formed by the accumulation of tracers at a transport barrier. Even if the pdf shows much scatter, making it difficult to fit a power law function to its left tail, it is clearly non-Gaussian.

Step size & Waiting time pdf

We have analyzed tracer motion by decomposing it into steps and waiting times. High velocity thresholds are needed filter out short-range motion and to obtain Lévy-like distributions. The step size pdf (Fig. 2, left) is expected to decay as $p \rightarrow \Delta x^{-(1+\alpha)}$ for large Δx . For a proper determination of α one would like to have a long power-law decay range, but we are limited by to the low spatial resolution of these simulations (100 radial grid points). So, while for low v_{TH} the local eddy motion dominates, for high v_{TH} this finite size effect becomes dominant. However, in-between, with $v_{TH} = 3 \cdot 10^4$ m/s, a relatively clear power-law is observed. Similar behaviour is observed for the waiting time pdf (Fig. 2, right), which decays as $\psi \rightarrow \Delta t^{-(1+\beta)}$ for large Δt . Here the power law range is longer than a decade, because the only limit for Δt is

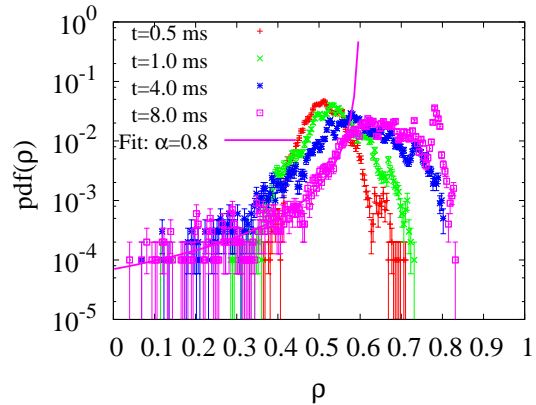


Figure 1: Radial distribution of tracers

the simulation length.

The best fits results are: $\alpha = 1.06 \pm 0.05$ and $\beta = 0.537 \pm 0.007$.

The measurement of H : Lagrangian Correlation and Structure Function

We have also determined H by means of the Lagrangian Correlation of velocities. The Rescaled Range (R/S) technique [4] provides a suitable algorithm for this purpose.

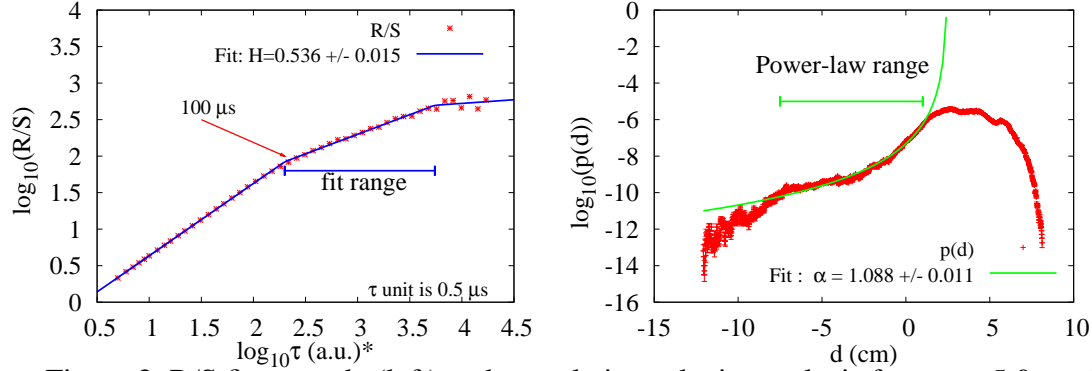


Figure 3: R/S fit example (left) and cumulative velocity analysis for $\tau_M = 5.0$ ms (right).

We evaluated $R(n)/S(n)$ for a range of different time intervals τ_n for each single tracer trajectory. In a range of τ_n values one expects to find: $\langle R(n)/S(n) \rangle \rightarrow \tau_n^H$ (e.g. Fig. 3, left). To obtain H , we fitted the R/S data to three connected power law sections. For time lags shorter than the turbulence decorrelation time ($t_d \sim 100 \mu$ s), we find $H \approx 1$; for large lags ($\tau \sim \tau_{Tot}$), $H \approx 0$, while in the intermediate region ($t_d < \tau \ll \tau_{Tot}$), $\langle H \rangle = 0.52 \pm 0.05$.

Another approach to the analysis of velocity correlations is the study of the distribution $p(d)$ of the total displacement d in a fixed time τ_M [5]. Long range correlations can be detected for large τ_M , however finite size effects occur for lag times similar to τ_{Tot} . This distribution is expected to behave as usual for large d : $p \rightarrow d^{-(1+\alpha)}$. Because of the finite size effect and the drift, again only the inward tail of the pdf is useful, and we find $\alpha = 1.089 \pm 0.011$ (Fig. 3, right). Note the similarity between Fig. 3, right and Fig. 1, which indicates a close match between individual and collective motion.

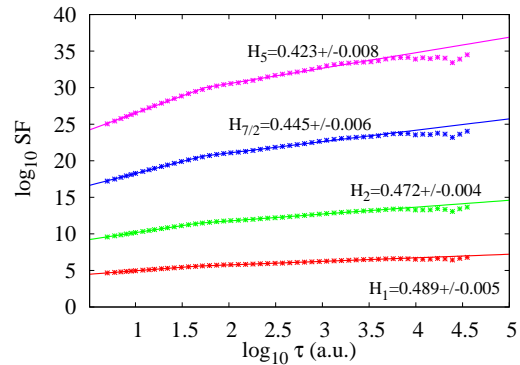


Figure 4: SF fit examples for different ν values

We have also computed the ν -order ($\nu = 1, \frac{3}{2}, 2, \dots, 5$) generalised structure function (SF) [6] for the radial velocity (Fig. 4), and found that it scales as a power law $S_\nu(\tau) = C_\nu \tau^{\nu \cdot H}$ in the

time range $\tau_1 < \tau < \tau_2$. To calculate H , we fit $S_v(\tau)$ discarding large values of τ ($\log_{10}(\tau) > 3.7$) by two connected power laws. Note that the slope changes approximately at the same lags as in the R/S plot. H is fairly constant with v . Its mean value is $\langle H \rangle = 0.452 \pm 0.019$.

The importance of the safety factor profile

We have detected a clear correlation between the q -profile and the tracer motion. The mean waiting time $\langle \tau \rangle(q)$ changes sharply near some low-order rational values: $q = \frac{3}{2}, 2, \frac{5}{2}, \frac{11}{4}, 3$ (Fig. 5(b)). Analogous behaviour is observed for $\langle \Delta r^2 \rangle$ at $q = 2, \frac{5}{2}$ (Fig. 5(c)). For higher v_{TH} this effect is enhanced. The corresponding mixing length diffusion coefficient shows a non-trivial structure with peaks and sharp slope variations close to the same q values (Fig. 5(a)), independently of v_{TH} , vaguely reminiscent of the phenomenological q -comb model [7].

Conclusions

Different analysis techniques were used for the characterisation of the radial motion of tracers in CUTIE, with consistent results. Interestingly, even if the motion is diffusive on average ($H \approx \frac{1}{2}$), it is clearly non-Gaussian and non-Markovian, since $\alpha \approx 1$ and $\beta \approx \frac{1}{2}$. The presence of internal transport barriers associated with some rational surfaces may be related to this phenomenon.

References

- [1] A. Thyagaraja, P. Knight, M. R. de Baar *et al.*, *Phys Plasmas* **12** 090907 (2005).
- [2] R. Sánchez, B. Ph. van Milligen and B. Carreras, *Phys Plasmas* **12** 056105 (2005).
- [3] B. Ph. van Milligen, R. Sánchez and B. Carreras, *Phys. Plasmas* **11** 2272 (2004).
- [4] B. Carreras, B. Ph. van Milligen *et al.*, *Phys. Rev. Lett.* **80** 4438 (1998).
- [5] R. Sánchez, B. Carreras *et al.*, *Phys. Rev. E* **74** 016305 (2006).
- [6] C. Yu, M. Gilmore *et al.*, *Phys. Plasmas* **10** 2772 (2003).
- [7] N. J. Lopes Cardozo, G. M. D. Hogeweij *et al.*, *Plasma Phys. Control. Fusion* **39** B303 (1997).

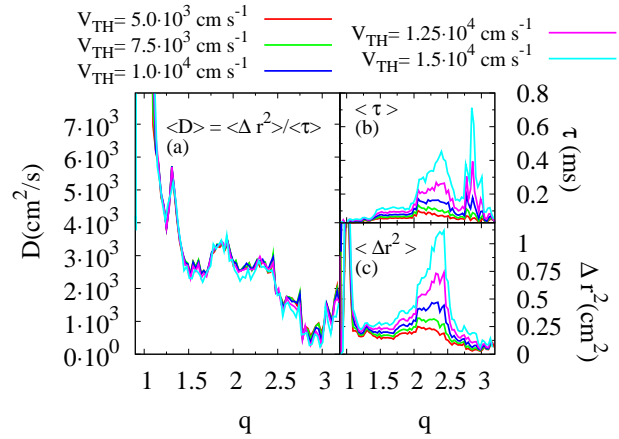


Figure 5: q has influence on transport